Anodic and Cathodic Protection Assessment on Chloride Molten Salts for the Next Generation of CSP Plants

Angel G. Fernández [a], Luisa F. Cabeza [b]

GREiA Research Group, INSPIRES Research Centre, Universitat de Lleida, Pere de Cabrera s/n, 25001-Lleida, Spain,
[a] angel.fernandez@diei.udl.cat
[b] lcabeza@diei.udl.cat

Abstract. The prevention of high-temperature corrosion on containment materials plays a critical role, and a corrosion mitigation plan is needed to achieve the target plant lifetime of 30 years. This paper analyzed two mitigation corrosion strategies (anodic and cathodic protection) in a eutectic ternary chloride molten salt, composed by 20.4wt.% KCl + 55.1wt.% $MgCl_2$ + 24.5wt.% NaCl. The corrosion mechanism and corrosion rates were obtained through electrochemical impedance spectroscopy (EIS). Ni base alloys generate a protective scale layer (anodic protection) during 8 hours of immersion with a corrosion rate of 6.34 mm/year (In702) and 3.12 mm/year (HR224). Monitoring corrosion results were confirmed by scanning electron microscopy (SEM) and X-ray diffraction (XRD), obtaining alumina and chromia protective layers.

INTRODUCTION

Molten salt technology using nitrate salts (the so-called solar salt) as thermal energy storage material is the current state-of-the-art of concentrated solar power technology; on the other hand power tower central receivers are currently limited by the maximum operating temperature of their working fluid, molten salts. The limit of solar salt (60wt.% $NaNO_3$ + 40wt.% KNO_3) thermal stability is around 565°C when ambient air is used as cover gas. In order to obtain higher efficiency goals using molten salt technologies working at higher temperatures (e.g., 650°C to 750°C), a different salt chemistry is required for the new generation of CSP plants and chlorides molten salts could be a feasible option [1]. Because of their low cost and high decomposition temperature, molten chlorides are considered good candidates. However, these molten salts introduce a set of technological and engineering challenges because of their very corrosiveness to typical containment materials. Corrosion mitigation could solve the current issues related with the use of chloride salt at high temperature. In this study, the proposal of different corrosion mitigation strategies, based on anodic and cathodic protection, was evaluated, as well as the identification of the most corrosive impurities present in the ternary chloride salt composed by $MgCl_2$/KCl/NaCl (44.7/25.8/29.4 mol%). For this purpose, electrochemical impedance spectroscopy (EIS) tests were carried out at 720°C on austenitic stainless steel (AISI 304), austenitic alumina forming alloys (OC4, OCT), and Ni base alloys (HR224, Inconel 702).

ANODIC PROTECTION

Anodic protection is a corrosion mitigation strategy that controls the corrosion rate of the surface to be protected the anode of an electrochemical cell. The initial reaction of the anode is usually accompanied by surface passivation which stops further reaction hence corrosion.

During last years, the proposal of alumina forming alloys (AFA) as storage container material saw a significant increase due to their better corrosion resistant behavior obtained by the formation of the alumina protective layers compared to chromia that is usually used in commercial stainless steel [2,3]. In the preliminary tests, a materials screening was carried out, testing stainless steels (AISI 304), austenitic forming alumina alloys (AFA OC-4, OC-T) and Ni base materials (HR224, In702), with the chemical composition shown in Table 1.

TABLE 1. Chemical composition of material immersed in chloride molten salt

In this paper only results obtained for HR224 and In702 are shown.

Steels	Weight (%)							
	Al	**Mn**	**Ni**	**Cr**	**Mo**	**Ti**	**Nb**	**Fe**
AISI 304	-	1.7	8.04	18.28	0.27	0.01	0.008	Balance
OC-4	3.5	2	25	14	2	0.1	2.5	Balance
OC-T	3	-	35	14	-	2	3	Balance
In 702	3	-	75	15	-	-	-	2
HR224	3.2	-	47	21	-	-	-	27.5

CATHODIC PROTECTION

Cathodic protection was proposed in the literature to mitigate corrosion of superalloys in molten salts. At a high level, a sacrificial metal that more easily “corrodes” is used to prevent corrosion of the super alloy or its components.

Because the corrosion reaction kinetics are so fast and the means to reduce mass transfer (without drastically change of the metal or salt composition/properties) might not be readily available, a key strategy to mitigate corrosion is to inhibit corrosion at the thermodynamic level. The reduction potential of various metal elements in chlorides can be easily obtained from the chloride Ellingham Diagram, which tells which metal species are stable in a certain chloride salt. By adding Mg metal into the molten $MgCl_2$-KCl mixture at a temperature higher than the melting point of Mg where Mg solubility is sufficiently high [5], the reduction potential of the alloy components can be shifted by more than 0.5 V such that both Cr^{2+} and Cr^{3+} are less stable than the cations in the molten-salt mixture. The most thermodynamically stable form of chromium in the superalloy is hence the metallic chromium, meaning that oxidation of chromium will not occur.

Because corrosion is a complicated subject of study that is specific to environment (e.g., isothermal vs. non-isothermal, stagnant vs. flowing condition of the corrosion liquid), multidimensional considerations must be given. Mehrabadi et al. [6,7] built a 3-D model that uses computational fluid dynamics (CFD) to account for electrochemical kinetics and incorporates the impacts of thermal gradients and fluid flow and effects of Mg corrosion inhibitor. The corrosion rates of Haynes 230, Haynes 163, and Incoloy 800H were experimentally obtained as a function of wt% of Mg added (from 0 to 1.15%). In all three cases, the corrosion rates were significantly reduced and the results from experiments and modeling agreed very well. Specifically, the corrosion rate of Haynes 230 at 850°C was reduced 35 times to less than 15 μm/year with 1.15 wt.% Mg addition compared to the baseline test without Mg addition. In a recent paper, Choi et al. indicated that a reduction peak associated with hy-droxides vanished with addition of MgO. These results demonstrate the benefit and mechanism for redox potential control in this salt using dissolved Mg metal.

However the oxidation of Mg introduces several corrosion impurities in the molten salt environment that could change its thermal energy storage potential. Due to this fact, in this work, the addition of copper metal is proposed.

EXPERIMENTAL PROCEDURE

The molten salt tested was the eutectic mixture $MgCl_2$/NaCl/KCl (44.7/29.5/25.8 mol%, Sigma Aldrich 99%) at 720ºC under inert atmosphere (N_2). Electrochemical impedance tests were obtained in a frequency range between 100 kHz and 10 mHz. Linear polarization tests were carried out from a potential of -0.6 to 0.4 V of the OCP voltage. The scanning range is 0.005 V/s with steps of 0.00244 V.

Working electrode (WE) and reference-counter (RE-CE) electrodes were immersed in the molten salt (electrolyte) and the Open Circuit Potential (OCP) was measured using a potentiostat (Gamry 1010E) connected to the system through a Cr-Ni wire. The experimental set up is shown in Figure 1.

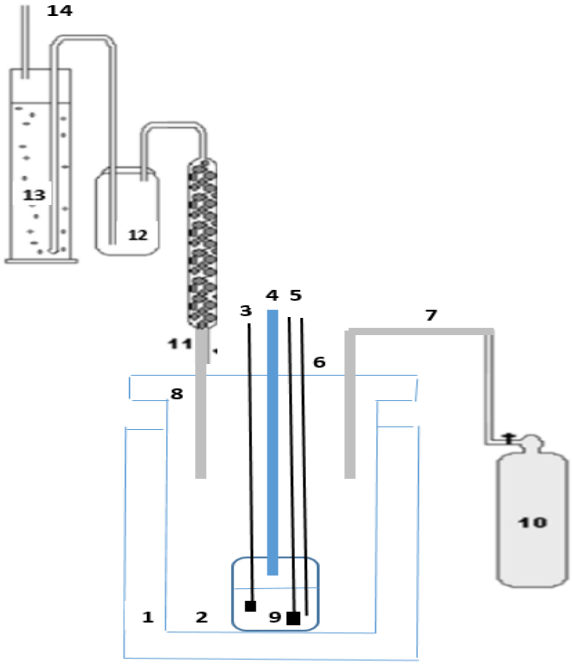

FIGURE 1. Experimental setup of electrochemical test in controlled atmosphere: 1: furnace; 2: molten salt reactor; 3: counter electrode, 4: thermocouple, 5: working electrode, 6: Reference electrode, 7: gas inlet, 9: molten salt, 10: carrier gas, 8: off-gas system (which consists of 11: MgO trap for chlorine; 12: moisture removal; 13: 1 M NaOH scrubber; and 14: gas exhaust.

Electrochemical techniques were used to monitor the corrosion mechanism in the materials tested. For this purpose, a electrochemical impedance test was carried out using the most common equivalent circuit used to model corrosion of bare metal, the Randles circuit [8]. The model can be used to estimate the polarization resistance from the impedance data [9]. Where R (Ω) is the uncompensated solution resistance, Rp is the polarization resistance, and CPE (Constant Phase Element) is the double layer capacitance. Nyquist plots are used to represent the real part of the impedance on the abscissa and the imaginary part thereof on the ordinate axis, both at different frequencies [10]. The semicircle obtained in the parallel RC circuit is used at higher values of Z' and represents the total impedance (Z) of the Randles circuit as:

$$Z = R_S + \frac{1}{\frac{1}{R_{ct}} + j\omega C_{dl}} \quad \text{[Eq. I]}$$

where R_s is the resistance of the solution, R_{ct} is the resistance to charge transfer, $j\omega$ is the imaginary radial frequency and C_{dl} is the capacitance of the double layer.

Different authors [10,11] proposed equivalent circuits that match to the main corrosion processes obtained in a molten salt environment at high temperature, obtaining different case scenarios, a localize corrosion model, porous layer or protective layer model.

After the EIS tests, a linear polarization resistance (LPR) test was carried out. The corrosion density current, i_{corr}, and the corrosion potential, E_{corr}, were determined from the extrapolation of the Tafel curve. The corrosion rate (CR) can be estimated through the Butler-Volmer equation showed in Eq. II:

$$CR = \frac{i_{corr} \cdot K}{\rho_{alloy} \cdot \Sigma\left(\frac{f_i \cdot n_i}{MW_i}\right)} \qquad \text{[Eq. II]}$$

where K is a correlation constant that defines the units of CR (3272 for CR in mm/year), ρ_{alloy} is the alloy density (g/cm^3), f_i is the mole fraction of the element i in the alloy, n_i is the number of electrons that are transferred in element i and MW_i is the atomic weight of element i.

RESULTS

Nyquist plots for HR224 alloy are shown in Figure 2. The equivalent circuit obtained at 1 hour (blue line) of immersion showed a localized corrosion model, nevertheless, after 3 and 5 hours a protective corrosion model was detected. Results for equivalent circuits elements are shown in Table 2. These results were confirmed by SEM (Figure 3), obtaining an internal oxidation (B analysis Figure 5 right) with higher Cr content. The outer layer in steel surface showed the formation of a protective layer formed by Fe-Cr-Al.

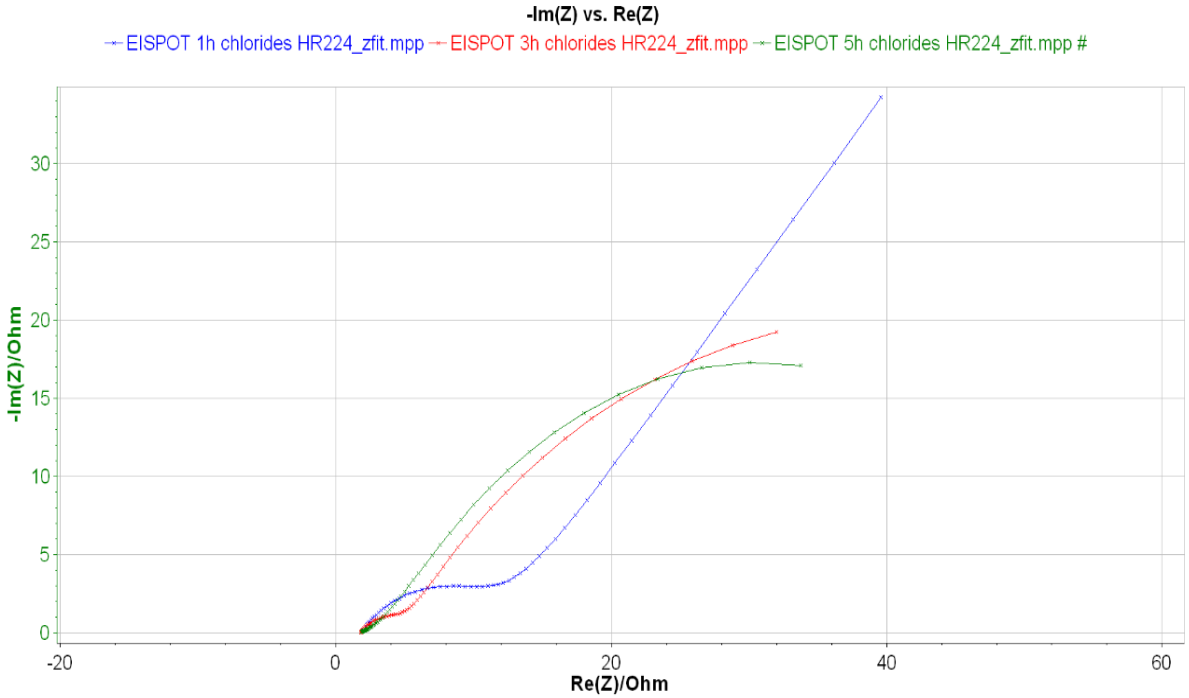

FIGURE 2. Nyquist diagram of HR224 immersed in ternary chloride molten salt at 1, 3 and 5 hours

TABLE 2. Electrochemical parameters obtained for EIS tests in hr224 alloy

Element	**R1 (Ohm)**	**Q2 (F/s)**	**R2 (Ohm)**	**Q3 (F/s)**	**R3 (Ohm)**	**Equivalent circuit**
1 h	1.812	4.87e-3	11.06	0.104	0.144	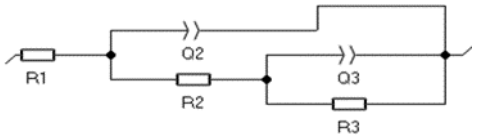
Element	**R3 (Ohm)**	**Q1 (F/s)**	**R5 (Ohm)**	**Q2 (F/s)**	**R7 (Ohm)**	
3 h	1.785	0.014	3.293	0.123	72.56	
5 h	1.71	0.166	55.4	0.257	74.11	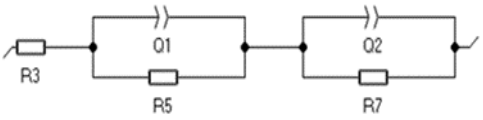

Element (wt.%)	Fe	Cr	Mg	O	Cl	Al	Ni
A	20.73	12.74	34.72	6.87	17.6	1.74	5.61
B	16.05	19.47	1.87	3.14	4.45	2.24	15.7

Element (wt.%)	Fe	Cr	Mg	O	Cl	Al
A	25.70	43.37	4.51	17.9	4.14	4.33
B	1.95	86.73	-	10.6	-	0.71

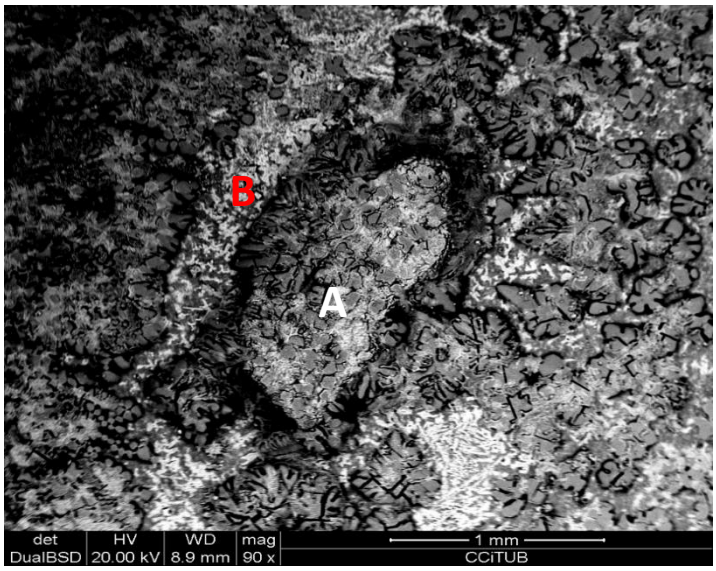

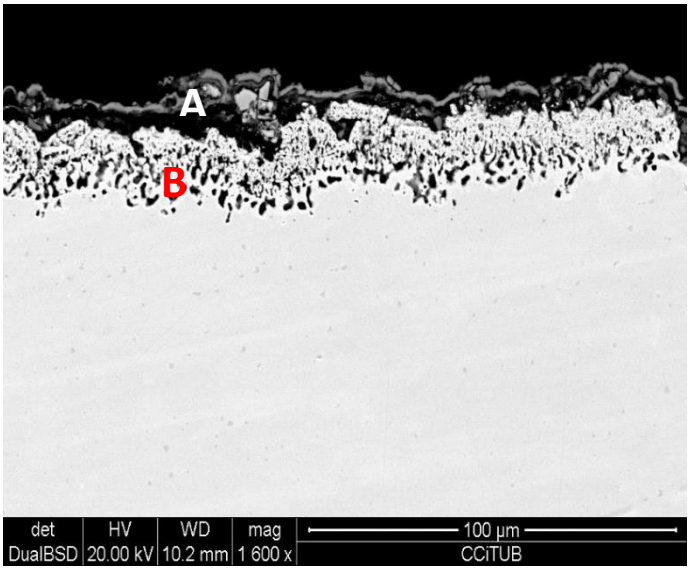

FIGURE 3. Top view (left) and cross section (right) images for HR224 immersed in ternary chloride molten salt during 8 h at 720ºC and EDX analysis

Last material tested was In702, showing a similar behaviour as the previous one, obtaining a localized corrosion model at 1 hour of immersion in ternary chloride molten salt and a protective layer corrosion model up 3 hours of corrosion test. Nyquist plots and equivalent circuits elements are shown in Figure 4 and Table 3. The corrosion mechanisms obtained at the end of the immersion test were confirmed by SEM (Figure 5). In this case, a protective layer of 8.93 microns with content in Fe-Ni-Cr-O-Al was detected.

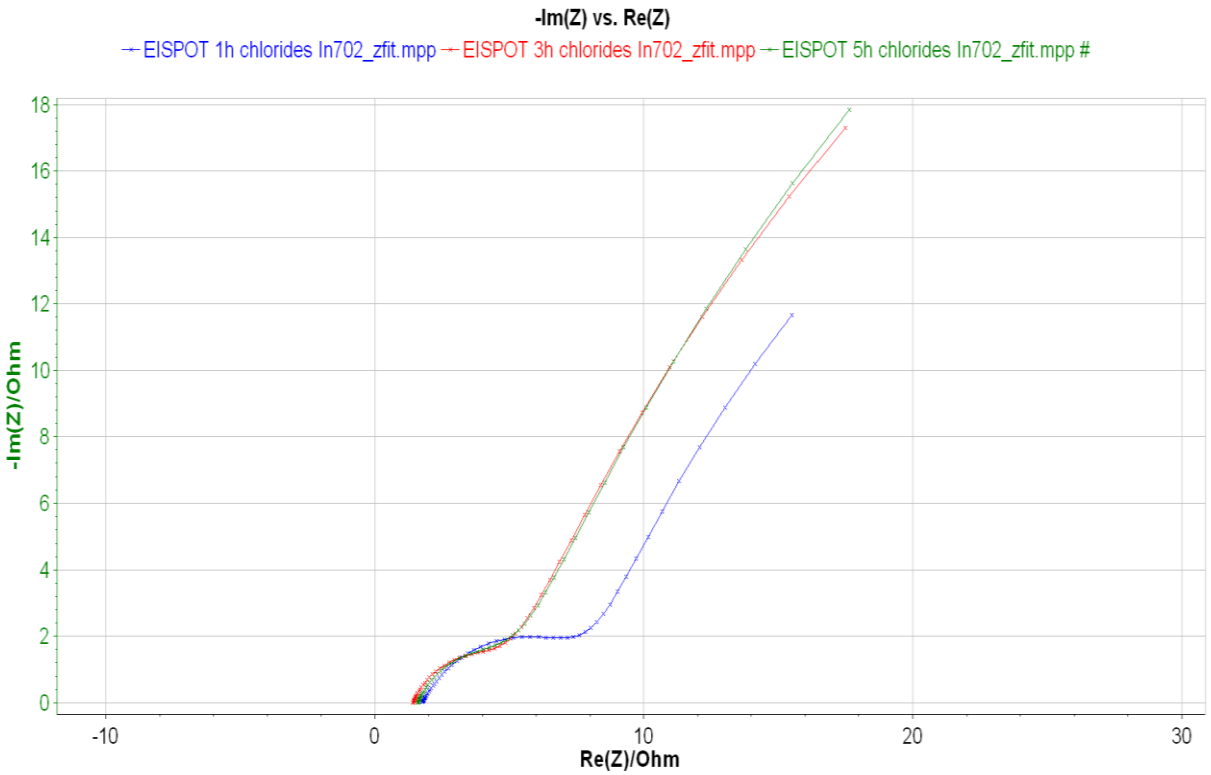

FIGURE 4. Nyquist diagram of In702 immersed in ternary chloride molten salt at 1, 3 and 5.hours

Table 3. Electrochemical parameters obtained for EIS tests in In702 alloy

Element	**R1 (Ohm)**	**Q2 (F/s)**	**R2 (Ohm)**	**Q3 (F/s)**	**R3 (Ohm)**	**Equivalent circuit**
1 h	1.762	0.026	7.029	0.484	69.58	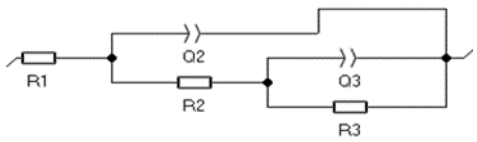
Element	**R3 (Ohm)**	**Q1 (F/s)**	**R5 (Ohm)**	**Q2 (F/s)**	**R7 (Ohm)**	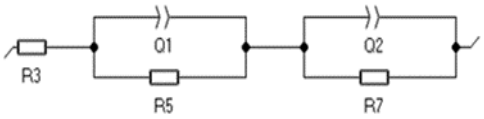
3 h	1.421	0.301	107.6	0.034	3.472	
5 h	1.604	0.041	3.536	0.303	115.7	

Element (Wt.%)	Fe	Cr	Mg	O	Cl	Al	Ni
A	5.24	5.06	30.53	15.03	7.55	6.24	30.2
B	16.64	3.86	2.55	2.20	0.5	-	74.26

Element (Wt.%)	Fe	Cr	O	Al	Ni
A	1.27	11.3	1.05	2.21	84.33

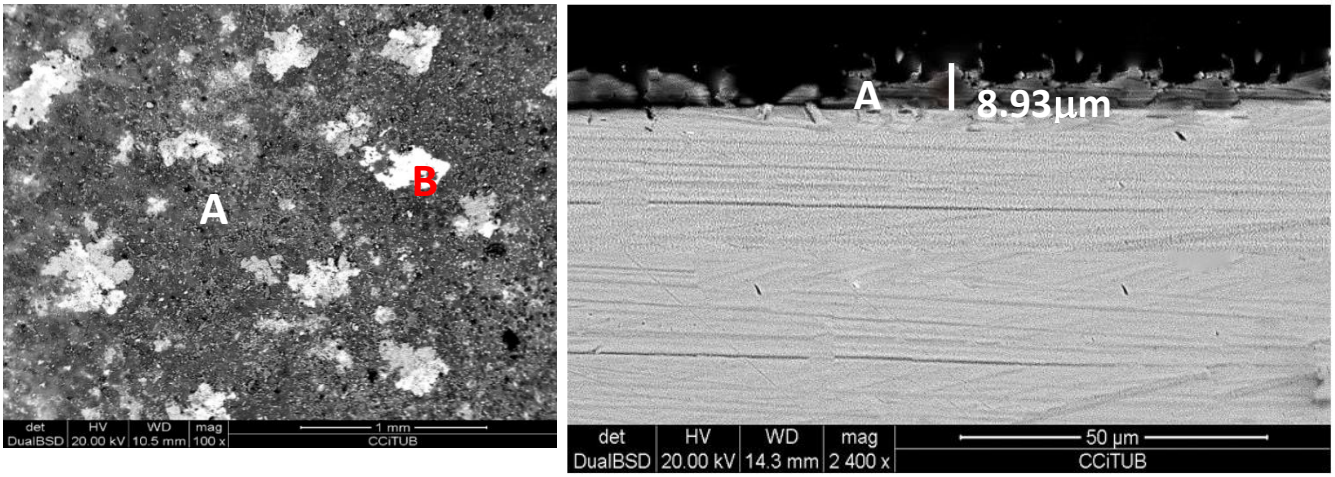

FIGURE 5. Top view (left) and cross section (right) images for In702 immersed in ternary chloride molten salt during 8h at 720ºC and EDX analysis

In order to confirm the corrosion layer composition obtained in the materials surface, a XRD analysis was carried out in all the materials tested. The chemical compounds obtained in the alloys immersed in chloride molten salts along with the different thermal treatment performed are shown in Table 4. Alumina protective layers were obtained for HR224 and In702, confirming the better corrosion resistance obtained in these materials when in contact with chloride molten salt and the corrosion mechanism detected by EIS and SEM.

TABLE 4. Corrosion products identified by XRD analysis on AISI304, HR224 and In702 after exposure to the salt mixture at 720 ºC for 8 h.

Salt mixture	**Material**	**Corrosion Products**	**Reference Pattern**
$MgCl_2$/NaCl/KCl (55.1 wt.% - 24.5 wt.% - 20.4 wt.%)	HR224	Al_2O_3 $MgCr_2O_4$	00-047-1292 01-082-1529
	In702	$MgAl_2O_4$ MgO NaCl	00-033-0853 01-087-0651 00-005-0628

Anodic protection test results are shown in Table 5.

TABLE 5. Electrochemical parameters and corrosion rates obtained for LPR test in the materials tested

Alloys	**Ecorr (mV)**	**Icorr (mA)**	**βc (mV)**	**βa (mV)**	**A (cm^2)**	**CR (mm/year)**
HR224	-97.609	2442.67	336.1	325.7	6.75	3.12
In702	-197.78	2876.55	338.6	1021.9	4.26	6.34

The linear polarization resistance technique was applied in the materials at 720ºC after 8 hours of immersion, obtaining a corrosion rate of 3.12 and 6.34 mm/year for HR224 and In702, respectively.

The best corrosion resistance was obtained for HR224 in concordance with EIS results (protective layer model) and XRD/SEM results, where a protective layer formed by Al_2O_3 and $MgCr_2O_4$ were detected in the steel surface.

Preliminary results obtained for cathodic protection using copper metal showed an important reduction in the corrosion rate obtained for HR224.

CONCLUSIONS

Anodic and cathodic protection techniques were studied to mitigate corrosion in chloride molten salts and linear polarization resistance technique was successfully applied in the materials tested and a down selection of materials was complete. The best corrosion resistance was obtained for HR224 alloy, obtaining an alumina protective layer, detected by electrochemical impedance spectroscopy and confirmed by SEM and XRD analysis. It is important to highlight that this alloy also showed an internal oxidation with higher chromium content forming a protective barrier composed by $MgCr_2O_4$, detected by XRD analysis. In a future research, longer exposure times will be carried out in HR224 trying to reduce the corrosion rate obtained.

ACKNOWLEDGEMENTS

Angel G. Fernández wants to acknowledge the financial support from the European Union's Horizon 2020 research and innovation programme under the Marie Sklodowska-Curie grant No 712949 (TECNIOspring PLUS) and from the Agency for Business Competitiveness of the Government of Catalonia. This work was partially funded by the Ministerio de Ciencia, Innovación y Universidades de España (RTI2018-093849-B-C31). The authors would like to thank the Catalan Government for the quality accreditation given to their research group GREiA (2017 SGR 1537). GREiA is a certified agent TECNIO in the category of technology developers from the Government of Catalonia. This work is partially supported by ICREA under the ICREA Academia programme.

REFERENCES

1. M. Mehos, C.T., J. Vidal, M. Wagner, Z. Ma, C. Ho, W. Kolb, C. Andraka and A. Kruizenga, Concentrating Solar Power Gen3 Demonstration Roadmap. Technical Report, NREL/TP-5500-67464, 2017.
2. Brady, M.P., Effects of minor alloy additions and oxidation temperature on protective alumina scale formation in creep-resistant austenitic stainless steels. Scripta Materialia, 2007. 57: p. 1117-1120.
3. Brady, M.P., Co-optimization of wrought alumina-forming austenitic stainless steel composition ranges for high-temperature creep and oxidation/corrosion resistance. Materials Science & Engineering A, 2014. 590: p. 101-115.
4. M. Krumpelt, J.F., I. Johnson, The Reaction of Magnesium Metal with Magnesium Chloride. J. Phys. Chem., 1968. 72: p. 506-511
5. M. Krumpelt, J. Fischer, and I. Johnson, "The Reaction of Magnesium Metal with Magnesium Chloride," J. Phys. Chem., 1968, 72, p. 506–511.
6. Mehrabadi, J. W. Weidner, B. Garcia-Diaz, M. Martinez-Rodriguez, L. Olson, and S. Shimpalee, "Modeling the Effect of Cathodic Protection on Superalloys Inside High Temperature Molten Salt Systems," J. Electrochem. Soc., 2017, 164, p. 171–179.

7. B. Mehrabadi, J. W. Weidner, B. Garcia-Diaz, M. Martinez-Rodriguez, L. Olson, and S. Shimpalee, “Multidimensional Modeling of Nickel Alloy Corrosion inside High Temperature Molten Salt Systems,” J. Electrochem. Soc., 2016, 163, p. 830–838.
8. Macdonald, D., Reflections on the history of electrochemical impedance spectroscopy. Electrochimica Acta, 2006, 51: p. 1376-1388.
9. Kisza, A., The capacitance of the diffuse layer of electric double layer of electrodes in molten salts. Electrochimica Acta, 2006. 51: p. 2315-2321.
10. Mark E. Orazem, An integrated approach to electrochemical impedance spectroscopy. Electrochimica Acta, 2008. 53: p. 7360–7366.
11. Zeng, C.L., W. Wang, and W.T. Wu, Electrochemical impedance models for molten salt corrosion. Corrosion Science, 2001, 43: p. 787-801.